ACS SENSORS

Letter

pubs.acs.org/acssensors

^{15}N Hyperpolarization of Imidazole-$^{15}N_2$ for Magnetic Resonance pH Sensing via SABRE-SHEATH

Roman V. Shchepin,[†] Danila A. Barskiy,[†] Aaron M. Coffey,[†] Thomas Theis,[∥] Fan Shi,[⊥] Warren S. Warren,[∥] Boyd M. Goodson,[⊥,#] and Eduard Y. Chekmenev*[,†,‡,§,¶]

[†]Vanderbilt University Institute of Imaging Science (VUIIS), Department of Radiology, [‡]Department of Biomedical Engineering, and [§]Vanderbilt-Ingram Cancer Center (VICC), Vanderbilt University, Nashville, Tennessee 37232-2310, United States

[∥]Department of Chemistry, Duke University, Durham, North Carolina 27708, United States

[⊥]Department of Chemistry and Biochemistry and [#]Materials Technology Center, Southern Illinois University, Carbondale, Illinois 62901, United States

[¶]Russian Academy of Sciences, Moscow, Leninskiy Prospekt 14, 119991, Russia

Supporting Information

ABSTRACT: ^{15}N nuclear spins of imidazole-$^{15}N_2$ were hyperpolarized using NMR signal amplification by reversible exchange in shield enables alignment transfer to heteronuclei (SABRE-SHEATH). A ^{15}N NMR signal enhancement of ∼2000-fold at 9.4 T is reported using parahydrogen gas (∼50% para-) and ∼0.1 M imidazole-$^{15}N_2$ in methanol:aqueous buffer (∼1:1). Proton binding to a ^{15}N site of imidazole occurs at physiological pH (pK_a ∼ 7.0), and the binding event changes the ^{15}N isotropic chemical shift by ∼30 ppm. These properties are ideal for in vivo pH sensing. Additionally, imidazoles have low toxicity and are readily incorporated into a wide range of biomolecules. ^{15}N-Imidazole SABRE-SHEATH hyperpolarization potentially enables pH sensing on scales ranging from peptide and protein molecules to living organisms.

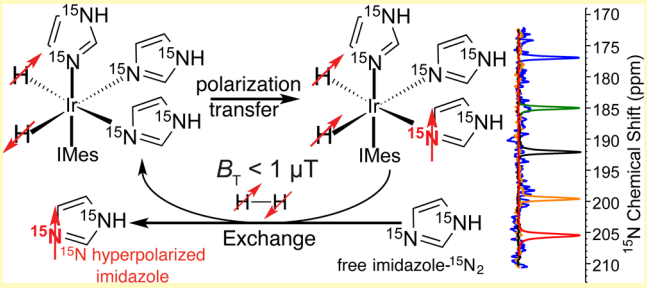

KEYWORDS: *NMR, hyperpolarization, parahydrogen, imidazole, pH sensing, ^{15}N, chemical shift*

Spectral sensing or imaging of local pH variances in vivo has been of long-standing interest for characterizing a host of pathological conditions, including various cancers.[1−6] For example, a variety of MR-based approaches using both exogenous and endogenous agents (e.g., refs 6−17) have been investigated as less invasive alternatives to using microelectrode probes.[6] However, sensitivity presents a significant challenge to otherwise powerful MR-based methods due to the typically low concentrations of probe molecules compared to water in vivo.

One way to combat such MR sensitivity limitations is hyperpolarization. NMR hyperpolarization techniques significantly enhance nuclear spin polarization (P), resulting in large gains in NMR signal.[18−20] One such approach is signal amplification by reversible exchange (SABRE), a technique that relies on exchange of parahydrogen (*para*-H_2) and to-be-hyperpolarized substrate molecules on a catalyst[21−23]—in solutions or in "neat" liquids.[24] Polarization of target nuclear spins (e.g., ^{1}H,[21] ^{15}N,[25,26] or ^{31}P[27]) occurs spontaneously when the applied static magnetic field B_T is "matched" to the corresponding spin−spin couplings between the nascent *para*-H_2 hydride pair and the target nuclei (Figure 1a). Homonuclear (i.e., ^{1}H) SABRE was demonstrated first[21] using B_T in the mT range; the approach was later extended to heteronuclei (e.g., ^{15}N, ^{31}P, etc.) via SABRE in shield enabling alignment transfer to heteronuclei (SABRE-SHEATH[25]) utilizing B_T static fields in the μT range. Alternatives to spontaneous SABRE or SABRE-SHEATH include radiofrequency irradiation targeting level anti-crossings (LAC)[28] and low-irradiation generation of high tesla-SABRE (LIGHT-SABRE).[29] These RF-based approaches are attractive because they yield hyperpolarization directly in the magnet where detection takes place. However, the spontaneous/static-field approaches currently yield larger polarization levels, up to 10% P_{15N} (corresponding to >30 000-fold signal enhancement at 9.4 T). A key advantage of all SABRE hyperpolarization methods is their fast polarization buildup—achieving high P levels in only a few seconds. Moreover, spontaneous SABRE and SABRE-SHEATH are not instrumentally demanding and only require access to readily produced *para*-H_2 and a weak static magnetic field. Furthermore, SABRE-SHEATH addresses a critical challenge faced by all hyperpolarization techniques: Upon injection of hyperpolarized (HP) material into a system of interest, signals usually decay rapidly, with decay constants on the order of

Received: April 6, 2016
Accepted: April 14, 2016
Published: April 14, 2016

DOI: 10.1021/acssensors.6b00231
ACS Sens. 2016, 1, 640−644

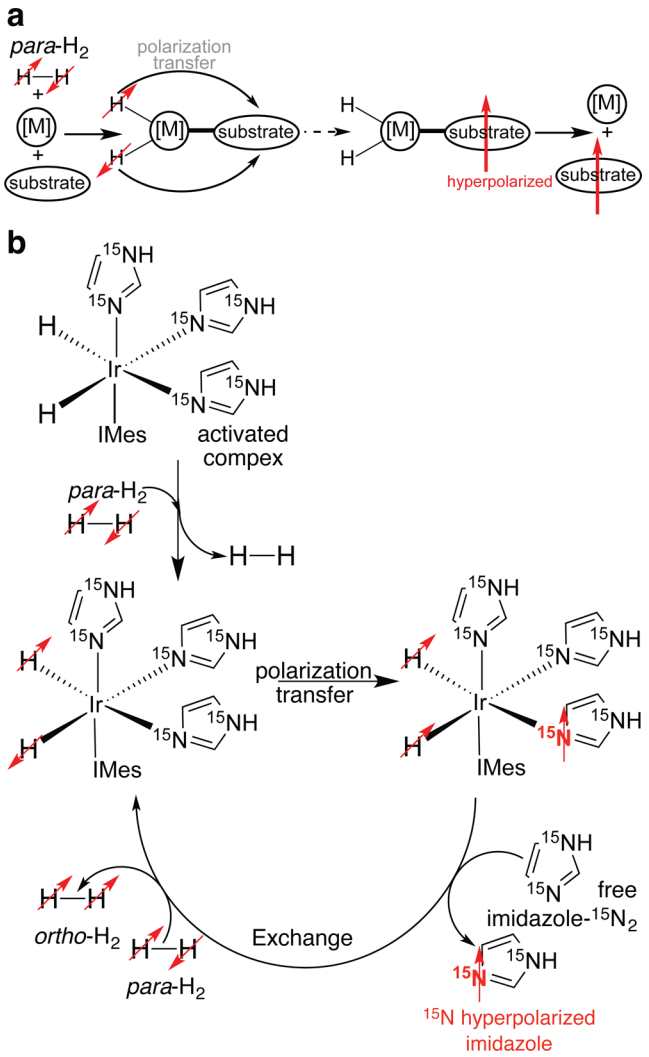

Figure 1. (a) Generalized scheme of SABRE and SABRE-SHEATH hyperpolarization processes. (b) Chemical structure of the activated Ir-IMes hexacoordinate complex after activation with H_2. The complex undergoes fast exchange with *para*-H_2 and free imidazole-$^{15}N_2$, which enables spontaneous polarization transfer from *para*-H_2 (in the form of Ir-hydrides) to ^{15}N nuclei of imidazole-$^{15}N_2$ in μT magnetic fields.[25,26]

seconds up to a minute. However, with SABRE-SHEATH, long-lived ^{15}N sites can be HP with relaxation time constants ranging from 1 min[26] to 10 min.[30] Furthermore, compared to ^{13}C enrichment of leading ^{13}C HP contrast agents (e.g., pyruvate-1-^{13}C[31,32]), spin labeling with ^{15}N uses relatively straightforward chemistry replacing N-sites in N-heterocycles with ^{15}N.[26,33]

The development of all hyperpolarization techniques has largely been driven by their use in biomedicine to image organ function and probe metabolic processes in vivo.[20,31,34,35] While several translational challenges of conventional SABRE have been addressed recently, i.e., demonstration of SABRE in aqueous media,[36−38] and implementation of heterogeneous SABRE catalysts,[39,40] most SABRE-hyperpolarized compounds studied to date have limited biological relevance (although nicotinamide,[21] pyrazinamide, and isoniazid[41] have been demonstrated). Recently, ^{15}N heterocycles have been shown to be potent for pH imaging.[42] In this case, hyperpolarization was performed with the well-established yet expensive dissolution-DNP (dynamic nuclear polarization)[43] modality and pH sensing was achieved by detecting changes in ^{15}N isotropic chemical shifts, which are >90 ppm for the protonated and deprotonated states of the ^{15}N-heterocycles.[42] As a result, ^{15}N isotropic chemical shifts of ^{15}N-hyperpolarized probes may be ideal reporters of in vivo pH. This approach has two key advantages compared to the current HP ^{13}C-bicarbonate pH sensing approach.[15] First, in vivo ^{15}N T_1 is significantly longer than that for ^{13}C (e.g., ∼10 s for ^{13}C bicarbonate[15]). Second, pH sensing using bicarbonate requires measurement and detection of both ^{13}C bicarbonate and its exchanging partner $^{13}CO_2$ via spectroscopic imaging (MRSI)—a demanding approach with respect to SNR, because the relative signal ratio of ^{13}C bicarbonate and $^{13}CO_2$ peaks must be measured with good precision, whereas this approach only requires accurate measurement of ^{15}N frequency, which can be performed with relatively low SNR.

A key challenge for in vivo pH sensing is a relatively narrow pH range for the extracellular compartments for most conditions of interest, requiring that a given pH probe provide a wide dynamic range of signal response over a relatively narrow range of pH values (i.e., ∼1.5 pH units). As a result, the pH sensor must have a pK_a close to physiological pH of ∼7. Initial studies of six-membered N-heterocycles (see Supporting Information Figure S1 and ref 42) identified only one somewhat suitable candidate: 2,6-lutidine,[42] with pK_a ∼ 6.6. However, 2,6-lutidine is not readily amenable to SABRE-SHEATH hyperpolarization.[24] The pK_a of imidazole is ∼7.0—a property that has already been exploited for in vivo tumor pH imaging via proton detection without hyperpolarization.[6,44] Therefore, imidazole nitrogen-15 sites are excellent candidates for ^{15}N HP pH sensing. Indeed, proton binding induces easily measured ^{15}N chemical shifts of ∼30 ppm (Figure 2).[45−47] Note that both ^{15}N sites have the same chemical shift in the deprotonated form because of fast proton hopping between these two sites in aqueous media.[45−47] In the protonated form, both ^{15}N sites are equivalent and have the same chemical shift. As a result, imidazole-$^{15}N_2$ is an excellent delivery vehicle, because its two ^{15}N sites carry twice the hyperpolarization payload of (single-site) pyridine derivatives.

Here, ^{15}N-SABRE-SHEATH hyperpolarization of imidazole-$^{15}N_2$ is demonstrated. Figure 2b shows the exchange process of imidazole-$^{15}N_2$ and *para*-H_2 gas on the activated Ir-IMes hexacoordinate complex of the most potent SABRE hyperpolarization catalyst to date.[23] As shown in Figure 2, ^{15}N signal enhancement ϵ_{15N} of ∼2000-fold is detected on each of the two ^{15}N sites in a methanol:aqueous (pH ∼ 12) buffer (∼1:1) solution of ∼0.1 M substrate utilizing only 50% *para*-H_2 gas and the hyperpolarization setup described previously.[26] Note the broad appearance of the HP NMR line in pure methanol-d_4 (Figure S3) owing to intermediate proton chemical exchange between the two ^{15}N sites described above; the ^{15}N NMR line is no longer broadened in aqueous solution (Figure 2d). The additional ^{15}N HP resonances (seen as narrow lines) are due to the presence of catalyst-bound ^{15}N imidazoles (Figure 2d inset and Figure S3a)—which have different pK_a values, protonation states, and proton exchange rates. If 100% *para*-H_2 would have been utilized (vs ∼50% *para*-H_2 utilized here), the enhancement would be effectively tripled to ϵ_{15N} ∼ 6000-fold, corresponding to P_{15N} ∼ 2%. Temperature and B_T[48] of the SABRE-SHEATH procedure were optimized to achieve the largest enhancements under our conditions. We note that unusually (for SABRE) high temperature (>340 K, Figure 2g)

DOI: 10.1021/acssensors.6b00231
ACS Sens. 2016, 1, 640−644

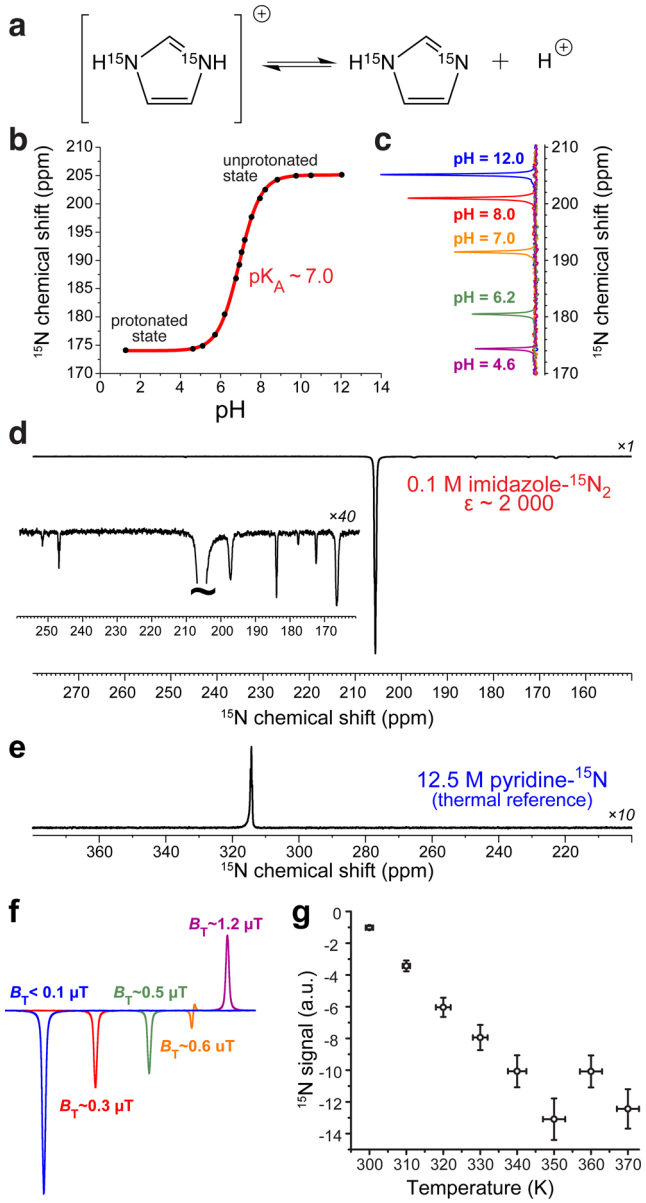

Figure 2. (a) Molecular diagram of imidazole-$^{15}N_2$ protonation; note that the effective molecular symmetry in unprotonated (due to fast proton hopping between two ^{15}N sites) and protonated states results in the same ^{15}N chemical shift of both sites. (b) Determination of imidazole-$^{15}N_2$ pK_a using isotropic ^{15}N chemical shift in aqueous solutions. (c) Selected (thermally-polarized) ^{15}N spectra of imidazole in water used for pK_a determination. (d) ^{15}N NMR spectrum of HP imidazole-$^{15}N_2$ (~0.1 M) in methanol:water (~1:1) produced via SABRE-SHEATH (B_T < 0.1 μT, [catalyst] ~ 4 mM); note the inset spectrum showing the other HP enlarged resonances: the large changes (i.e., ≥10 ppm) of a ^{15}N chemical shift of these species are caused by the imidazole position in the hexacoordinate complex (e.g., equatorial vs axial position, Figure 1b), binding state (e.g., free vs catalyst-bound states, Figure 1b),[25,26] and protonation states.[42] (e) ^{15}N spectrum of a ^{15}N signal reference. (f,g) SABRE-SHEATH optimization of magnetic transfer field B_T and temperature, respectively. All NMR spectra are recorded using a 400 MHz Bruker NMR spectrometer.

was found optimal for 15N SABRE-SHEATH in the aqueous medium (Figure 2f,g).

These results represent the highest payload (defined as the product of ^{15}N concentration and polarization) for any SABRE-hyperpolarized compounds with the exception of ^{15}N-nicotinamide (50 mM and P_{15N} ~ 11% at ~100% *para*-H_2 limit), which was achieved in pure methanol-d_4 using preactivation with pyridine,[33] whereas here, ^{15}N SABRE-SHEATH was performed in an aqueous medium, which is known to provide lower enhancements due to lower *para*-H_2 solubility.[37] A potential solution is a further significant increase of *para*-H_2 pressure (compared to ~6.5 atm used here), which could potentially enable significantly larger polarization levels,[24,26] e.g., P_{15N} ~ 10% or more. ^{15}N T_1 of imidazole-$^{15}N_2$ in methanol:aqueous (pH ~ 12) buffer (~1:1) solution in the presence of SABRE catalyst was 24 ± 1 s at 9.4 T, whereas further reduction of methanol fraction (to an estimated value of <10% by volume) resulted in a T_1 increase to 86 ± 2 s (Figure S2) indicating that the in vivo T_1 (with the absence of both alcohol and exchangeable catalyst) could potentially exceed 1 min.[49] The ^{15}N hyperpolarization lifetime could also be further enhanced via long-lived spin states and the use of lower magnetic fields.[30]

Motivated by potential biomedical translation, SABRE-SHEATH hyperpolarization of imidazole-$^{15}N_2$ in aqueous media was performed at several different pH values (below and above the pK_a, Figure 3) demonstrating that (i) ^{15}N chemical shift of the HP probe indeed changes by ~30 ppm, and (ii) the ^{15}N NMR resonances are sufficiently narrow to discriminate minute changes in pH in the physiologically relevant range. Therefore, this HP molecular probe can potentially enable in vivo pH sensing with an estimated ~15 ppm range covering pH range 6.5 to 7.5, and it should provide resolution of 0.1 unit of pH per 1.5 ppm of ^{15}N shift.

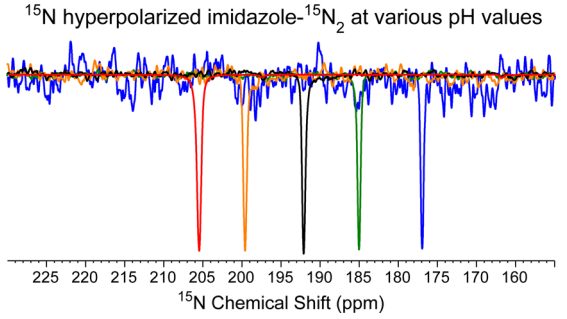

Figure 3. ^{15}N NMR spectra of imidazole-$^{15}N_2$ hyperpolarized via SABRE-SHEATH at various pH values (below and above pK_a) in aqueous solutions containing <50% methanol. Note a minor shift of ~2 ppm between resonances shown in Figure 2c (not color matched) and here due to temperature difference of ~40 °C.

Conventional ^1H-SABRE of methanol-d_4 solution yielded ε_H ~ 50−100-fold (Figure S3e), i.e., values lower than the corresponding ^{15}N enhancements (Figure S3a)—in agreement with previous ^{15}N SABRE-SHEATH studies of ^{15}N-pyridine.[26] Moreover, Figure S3d also shows in situ (or "high-field") SABRE ^1H NMR spectroscopy of imidazole-$^{15}N_2$ recorded inside a 9.4 T spectrometer (the spectrum was recorded approximately 2 s after *para*-H_2 bubbling (conducted at 9.4 T) was stopped—note (i) the partial SABRE signal enhancement of one of the imidazole protons, manifested as the signal with negative (emissive) phase—consistent with the previously described "high-field" SABRE effect;[50] and (ii) upfield ^1H signals from intermediate hydride species formed transiently during the catalyst activation process.[37] Taken together, the ^{15}N SABRE-SHEATH and ^1H SABRE results indicate that

DOI: 10.1021/acssensors.6b00231
ACS Sens. 2016, 1, 640−644

imidazole-$^{15}N_2$ reversible exchange (and SABRE in general) have the same key features as the most-studied SABRE substrate, pyridine.

While d-DNP could in principle be employed for hyperpolarization of imidazole-$^{15}N_2$, it is an instrumentationally demanding and expensive hyperpolarization technique, and DNP hyperpolarization processes for this class of compound typically require ∼2 h of polarization build-up.[42] ^{15}N SABRE-SHEATH allows preparation of HP imidazole-$^{15}N_2$ (and potentially other imidazole-based biomolecules) in less than a minute using a very simple experimental setup, paving the way to pH sensing (imaging and localized spectroscopy) in vivo. Furthermore, in combination with recent demonstrations of SABRE in aqueous media[36−38] and in "neat" liquids,[24] the presented work potentially enables the hyperpolarization of ^{15}N-imidazole moieties for structural and functional studies of peptides and proteins.[51,52]

■ ASSOCIATED CONTENT

Supporting Information

The Supporting Information is available free of charge on the ACS Publications website at DOI: 10.1021/acssensors.6b00231.

Table summarizing pK_a values; additional figures providing quantitative measurements of pK_a using ^{15}N NMR spectroscopy; additional experimental details and other supporting figures (PDF)

■ AUTHOR INFORMATION

Corresponding Author

*E-mail: eduard.chekmenev@vanderbilt.edu.

Notes

The authors declare no competing financial interest.

■ ACKNOWLEDGMENTS

This work was supported by NSF under grants CHE-1058727, CHE-1363008, CHE-1416268, and CHE-1416432, NIH (1R21EB018014, 1R21EB020323, and 2R15EB007074-02), DOD CDMRP BRP W81XWH-12-1-0159/BC112431, DOD PRMRP awards W81XWH-15-1-0271 and W81XWH-15-1-0272, T32 EB001628, and Exxon Mobil Knowledge Build.

■ REFERENCES

(1) Vaupel, P.; Kallinowski, F.; Okunieff, P. Blood Flow, Oxygen and Nutrient Supply, and Metabolic Microenvironment of Human Tumors: A Review. *Cancer Res.* **1989**, *49*, 6449−6465.

(2) Tannock, I. F.; Rotin, D. Acid pH in Tumors and Its Potential for Therapeutic Exploitation. *Cancer Res.* **1989**, *49*, 4373−4384.

(3) Martin, G. R.; Jain, R. K. Noninvasive Measurement of Interstitial pH Profiles in Normal and Neoplastic Tissue Using Fluorescence Ratio Imaging Microscopy. *Cancer Res.* **1994**, *54*, 5670−5674.

(4) Gerweck, L. E.; Seetharaman, K. Cellular pH Gradient in Tumor Versus Normal Tissue: Potential Exploitation for the Treatment of Cancer. *Cancer Res.* **1996**, *56*, 1194−1198.

(5) Carmeliet, P.; Jain, R. K. Angiogenesis in Cancer and Other Diseases. *Nature* **2000**, *407*, 249−257.

(6) Gillies, R. J.; Raghunand, N.; Garcia-Martin, M. L.; Gatenby, R. A. pH Imaging. *IEEE Eng. Med. Biol. Mag.* **2004**, *23*, 57−64.

(7) Saha, I.; Chaffee, K. E.; Duanmu, C.; Woods, B. M.; Stokes, A. M.; Buck, L. E.; Walkup, L. L.; Sattenapally, N.; Huggenvik, J.; Gao, Y.; et al. pH-Sensitive MR Responses Induced by Dendron-Functionalized SPIONs. *J. Phys. Chem. C* **2013**, *117*, 1893−1903.

(8) Vermathen, P.; Capizzano, A. A.; Maudsley, A. A. Administration and ^{1}H MRS Detection of Histidine in Human Brain: Application to in Vivo pH Measurement. *Magn. Reson. Med.* **2000**, *43*, 665−675.

(9) Zhou, J.; Payen, J.-F.; Wilson, D. A.; Traystman, R. J.; van Zijl, P. C. M. Using the Amide Proton Signals of Intracellular Proteins and Peptides to Detect pH Effects in MRI. *Nat. Med.* **2003**, *9*, 1085−1090.

(10) Stubbs, M.; Bhujwalla, Z. M.; Tozer, G. M.; Rodrigues, L. M.; Maxwell, R. J.; Morgan, R.; Howe, F. A.; Griffiths, J. R. An Assessment of ^{31}P MRS as a Method of Measuring pH in Rat Tumours. *NMR Biomed.* **1992**, *5*, 351−359.

(11) Gillies, R. J.; Liu, Z.; Bhujwalla, Z. P-31-MRS Measurements of Extracellular pH of Tumors Using 3-Aminopropylphosphonate. *Am. J. Physiol.* **1994**, *267*, C195−C203.

(12) Ackerman, J. J. H.; Soto, G. E.; Spees, W. M.; Zhu, Z.; Evelhoch, J. L. The NMR Chemical Shift pH Measurement Revisited: Analysis of Error and Modeling of a pH Dependent Reference. *Magn. Reson. Med.* **1996**, *36*, 674−683.

(13) Zhang, S.; Winter, P.; Wu, K.; Sherry, A. D. A Novel Europium(III)-Based MRI Contrast Agent. *J. Am. Chem. Soc.* **2001**, *123*, 1517−1518.

(14) Lowe, M. P.; Parker, D.; Reany, O.; Aime, S.; Botta, M.; Castellano, G.; Gianolio, E.; Pagliarin, R. pH-Dependent Modulation of Relaxivity and Luminescence in Macrocyclic Gadolinium and Europium Complexes Based on Reversible Intramolecular Sulfonamide Ligation. *J. Am. Chem. Soc.* **2001**, *123*, 7601−7609.

(15) Gallagher, F. A.; Kettunen, M. I.; Day, S. E.; Hu, D. E.; Ardenkjaer-Larsen, J. H.; in't Zandt, R.; Jensen, P. R.; Karlsson, M.; Golman, K.; Lerche, M. H.; et al. Magnetic Resonance Imaging of pH in Vivo Using Hyperpolarized C-13-Labelled Bicarbonate. *Nature* **2008**, *453*, 940−943.

(16) Raghunand, N.; Howison, C.; Sherry, A. D.; Zhang, S.; Gillies, R. J. Renal and Systemic pH Imaging by Contrast-Enhanced MRI. *Magn. Reson. Med.* **2003**, *49*, 249−257.

(17) Gianolio, E.; Maciocco, L.; Imperio, D.; Giovenzana, G. B.; Simonelli, F.; Abbas, K.; Bisi, G.; Aime, S. Dual MRI-SPECT Agent for pH-Mapping. *Chem. Commun.* **2011**, *47*, 1539−1541.

(18) Abragam, A.; Goldman, M. Principles of Dynamic Nuclear Polarization. *Rep. Prog. Phys.* **1978**, *41*, 395−467.

(19) Carver, T. R.; Slichter, C. P. Polarization of Nuclear Spins in Metals. *Phys. Rev.* **1953**, *92*, 212−213.

(20) Nikolaou, P.; Goodson, B. M.; Chekmenev, E. Y. NMR Hyperpolarization Techniques for Biomedicine. *Chem. - Eur. J.* **2015**, *21*, 3156−3166.

(21) Adams, R. W.; Aguilar, J. A.; Atkinson, K. D.; Cowley, M. J.; Elliott, P. I. P.; Duckett, S. B.; Green, G. G. R.; Khazal, I. G.; Lopez-Serrano, J.; Williamson, D. C. Reversible Interactions with Para-Hydrogen Enhance NMR Sensitivity by Polarization Transfer. *Science* **2009**, *323*, 1708−1711.

(22) Adams, R. W.; Duckett, S. B.; Green, R. A.; Williamson, D. C.; Green, G. G. R. A Theoretical Basis for Spontaneous Polarization Transfer in Non-Hydrogenative Parahydrogen-Induced Polarization. *J. Chem. Phys.* **2009**, *131*, 194505.

(23) Cowley, M. J.; Adams, R. W.; Atkinson, K. D.; Cockett, M. C. R.; Duckett, S. B.; Green, G. G. R.; Lohman, J. A. B.; Kerssebaum, R.; Kilgour, D.; Mewis, R. E. Iridium N-Heterocyclic Carbene Complexes as Efficient Catalysts for Magnetization Transfer from Para-Hydrogen. *J. Am. Chem. Soc.* **2011**, *133*, 6134−6137.

(24) Shchepin, R. V.; Truong, M. L.; Theis, T.; Coffey, A. M.; Shi, F.; Waddell, K. W.; Warren, W. S.; Goodson, B. M.; Chekmenev, E. Y. Hyperpolarization of "Neat" Liquids by NMR Signal Amplification by Reversible Exchange. *J. Phys. Chem. Lett.* **2015**, *6*, 1961−1967.

(25) Theis, T.; Truong, M. L.; Coffey, A. M.; Shchepin, R. V.; Waddell, K. W.; Shi, F.; Goodson, B. M.; Warren, W. S.; Chekmenev, E. Y. Microtesla SABRE Enables 10% Nitrogen-15 Nuclear Spin Polarization. *J. Am. Chem. Soc.* **2015**, *137*, 1404−1407.

(26) Truong, M. L.; Theis, T.; Coffey, A. M.; Shchepin, R. V.; Waddell, K. W.; Shi, F.; Goodson, B. M.; Warren, W. S.; Chekmenev, E. Y. ^{15}N Hyperpolarization by Reversible Exchange Using SABRE-SHEATH. *J. Phys. Chem. C* **2015**, *119*, 8786−8797.

DOI: 10.1021/acssensors.6b00231
ACS Sens. 2016, 1, 640−644

(27) Zhivonitko, V. V.; Skovpin, I. V.; Koptyug, I. V. Strong ^{31}P Nuclear Spin Hyperpolarization Produced Via Reversible Chemical Interaction with Parahydrogen. *Chem. Commun.* **2015**, *51*, 2506−2509.
(28) Pravdivtsev, A. N.; Yurkovskaya, A. V.; Vieth, H.-M.; Ivanov, K. L. Spin Mixing at Level Anti-Crossings in the Rotating Frame Makes High-Field SABRE Feasible. *Phys. Chem. Chem. Phys.* **2014**, *16*, 24672−24675.
(29) Theis, T.; Truong, M.; Coffey, A. M.; Chekmenev, E. Y.; Warren, W. S. LIGHT-SABRE Enables Efficient in-Magnet Catalytic Hyperpolarization. *J. Magn. Reson.* **2014**, *248*, 23−26.
(30) Theis, T.; Ortiz, G. X.; Logan, A. W. J.; Claytor, K. E.; Feng, Y.; Huhn, W. P.; Blum, V.; Malcolmson, S. J.; Chekmenev, E. Y.; Wang, Q.; et al. Direct and Cost-Efficient Hyperpolarization of Long-Lived Nuclear Spin States on Universal $^{15}N_2$-Diazirine Molecular Tags. *Sci. Adv.* **2016**, *2*, e1501438.
(31) Kurhanewicz, J.; Vigneron, D. B.; Brindle, K.; Chekmenev, E. Y.; Comment, A.; Cunningham, C. H.; DeBerardinis, R. J.; Green, G. G.; Leach, M. O.; Rajan, S. S.; et al. Analysis of Cancer Metabolism by Imaging Hyperpolarized Nuclei: Prospects for Translation to Clinical Research. *Neoplasia* **2011**, *13*, 81−97.
(32) Nelson, S. J.; Kurhanewicz, J.; Vigneron, D. B.; Larson, P. E. Z.; Harzstark, A. L.; Ferrone, M.; van Criekinge, M.; Chang, J. W.; Bok, R.; Park, I.; et al. Metabolic Imaging of Patients with Prostate Cancer Using Hyperpolarized 1-C-13 Pyruvate. *Sci. Transl. Med.* **2013**, *5*, 198ra108.
(33) Shchepin, R. V.; Barskiy, D. A.; Mikhaylov, D. M.; Chekmenev, E. Y. Efficient Synthesis of Nicotinamide-1-^{15}N for Ultrafast NMR Hyperpolarization Using Parahydrogen. *Bioconjugate Chem.* **2016**, DOI: 10.1021/acs.bioconjchem.6b00148.
(34) Brindle, K. M. Imaging Metabolism with Hyperpolarized ^{13}C-Labeled Cell Substrates. *J. Am. Chem. Soc.* **2015**, *137*, 6418−6427.
(35) Comment, A.; Merritt, M. E. Hyperpolarized Magnetic Resonance as a Sensitive Detector of Metabolic Function. *Biochemistry* **2014**, *53*, 7333−7357.
(36) Zeng, H.; Xu, J.; McMahon, M. T.; Lohman, J. A. B.; van Zijl, P. C. M. Achieving 1% NMR Polarization in Water in Less Than 1 min Using SABRE. *J. Magn. Reson.* **2014**, *246*, 119−121.
(37) Truong, M. L.; Shi, F.; He, P.; Yuan, B.; Plunkett, K. N.; Coffey, A. M.; Shchepin, R. V.; Barskiy, D. A.; Kovtunov, K. V.; Koptyug, I. V.; et al. Irreversible Catalyst Activation Enables Hyperpolarization and Water Solubility for NMR Signal Amplification by Reversible Exchange. *J. Phys. Chem. B* **2014**, *118*, 13882−13889.
(38) Hövener, J.-B.; Schwaderlapp, N.; Borowiak, R.; Lickert, T.; Duckett, S. B.; Mewis, R. E.; Adams, R. W.; Burns, M. J.; Highton, L. A. R.; Green, G. G. R.; et al. Toward Biocompatible Nuclear Hyperpolarization Using Signal Amplification by Reversible Exchange: Quantitative in Situ Spectroscopy and High-Field Imaging. *Anal. Chem.* **2014**, *86*, 1767−1774.
(39) Shi, F.; Coffey, A. M.; Waddell, K. W.; Chekmenev, E. Y.; Goodson, B. M. Heterogeneous Solution NMR Signal Amplification by Reversible Exchange. *Angew. Chem., Int. Ed.* **2014**, *53*, 7495−7498.
(40) Shi, F.; Coffey, A. M.; Waddell, K. W.; Chekmenev, E. Y.; Goodson, B. M. Nanoscale Catalysts for NMR Signal Enhancement by Reversible Exchange. *J. Phys. Chem. C* **2015**, *119*, 7525−7533.
(41) Zeng, H.; Xu, J.; Gillen, J.; McMahon, M. T.; Artemov, D.; Tyburn, J.-M.; Lohman, J. A. B.; Mewis, R. E.; Atkinson, K. D.; Green, G. G. R.; et al. Optimization of SABRE for Polarization of the Tuberculosis Drugs Pyrazinamide and Isoniazid. *J. Magn. Reson.* **2013**, *237*, 73−78.
(42) Jiang, W.; Lumata, L.; Chen, W.; Zhang, S.; Kovacs, Z.; Sherry, A. D.; Khemtong, C. Hyperpolarized ^{15}N-Pyridine Derivatives as pH-Sensitive MRI Agents. *Sci. Rep.* **2015**, *5*, 9104.
(43) Ardenkjaer-Larsen, J. H.; Fridlund, B.; Gram, A.; Hansson, G.; Hansson, L.; Lerche, M. H.; Servin, R.; Thaning, M.; Golman, K. Increase in Signal-to-Noise Ratio of > 10,000 Times in Liquid-State NMR. *Proc. Natl. Acad. Sci. U. S. A.* **2003**, *100*, 10158−10163.
(44) Hashim, A. I.; Zhang, X.; Wojtkowiak, J. W.; Gillies, R. J.; Martinez, G. V. Imaging pH and Metastasis. *NMR Biomed.* **2011**, *24*, 582−591.
(45) Alei, M.; Morgan, L. O.; Wageman, W. E. Nitrogen-15 Magnetic Resonance of Aqueous Imidazole and Zinc(II)-Imidazole Complexes. Evidence for Hexacoordination. *Inorg. Chem.* **1978**, *17*, 2288−2293.
(46) Alei, M.; Wageman, W. E.; Morgan, L. O. Nitrogen-15 Chemical Shifts for Imidazole in Aqueous Cadmium(2+) Solutions. *Inorg. Chem.* **1978**, *17*, 3314−3315.
(47) Alei, M.; Morgan, L. O.; Wageman, W. E.; Whaley, T. W. Ph-Dependence of N-15 NMR Shifts and Coupling Constants in Aqueous Imidazole and 1-Methylimidazole - Comments on Estimation of Tautomeric Equilibrium Constants for Aqueous Histidine. *J. Am. Chem. Soc.* **1980**, *102*, 2881−2887.
(48) Lloyd, L. S.; Asghar, A.; Burns, M. J.; Charlton, A.; Coombes, S.; Cowley, M. J.; Dear, G. J.; Duckett, S. B.; Genov, G. R.; Green, G. G. R.; et al. Hyperpolarisation through Reversible Interactions with Parahydrogen. *Catal. Sci. Technol.* **2014**, *4*, 3544−3554.
(49) Cudalbu, C.; Comment, A.; Kurdzesau, F.; van Heeswijk, R. B.; Uffmann, K.; Jannin, S.; Denisov, V.; Kirik, D.; Gruetter, R. Feasibility of in Vivo N-15 MRS Detection of Hyperpolarized N-15 Labeled Choline in Rats. *Phys. Chem. Chem. Phys.* **2010**, *12*, 5818−5823.
(50) Barskiy, D. A.; Kovtunov, K. V.; Koptyug, I. V.; He, P.; Groome, K. A.; Best, Q. A.; Shi, F.; Goodson, B. M.; Shchepin, R. V.; Coffey, A. M.; et al. The Feasibility of Formation and Kinetics of NMR Signal Amplification by Reversible Exchange (SABRE) at High Magnetic Field (9.4 T). *J. Am. Chem. Soc.* **2014**, *136*, 3322−3325.
(51) Miao, Y.; Cross, T. A.; Fu, R. Differentiation of Histidine Tautomeric States Using ^{15}N Selectively Filtered ^{13}C Solid-State NMR Spectroscopy. *J. Magn. Reson.* **2014**, *245*, 105−109.
(52) Hu, F.; Luo, W.; Hong, M. Mechanisms of Proton Conduction and Gating in Influenza M2 Proton Channels from Solid-State NMR. *Science* **2010**, *330*, 505−508.

DOI: 10.1021/acssensors.6b00231
ACS Sens. 2016, 1, 640−644